International Journal of Engineering Science 205 (2024) 104152

Contents lists available at ScienceDirect

International Journal of Engineering Science

journal homepage: www.elsevier.com/locate/ijengsci

Full length article

# On the refined boundary condition at the edge of a thin elastic strip supported by a Winkler-type foundation under antiplane shear deformation

Ludmila Prikazchikova [a], Evgeniya Nolde [b], Wiktoria Miszuris [c,*], Julius Kaplunov [a]

[a] Keele University, School of Computer Science and Mathematics, Keele, ST5 5BG, Staffordshire, UK
[b] Brunel University London, Department of Mathematics, CEDPS, Uxbridge, UB8 3PH, Middlesex, UK
[c] Aberystwyth University, Department of Mathematics, Aberystwyth, SY23 3BZ, Wales, UK

ARTICLE INFO

*Keywords:*
Elastic strip
Antiplane shear
Asymptotic
Saint–Venant's principle
Decay conditions
Low-dimensional theory
Winkler foundation
Boundary layer
Interior solution

ABSTRACT

The derivation of the boundary conditions is the most challenging part of the asymptotic techniques underlying low-dimensional models for thin elastic structures. At the moment, these techniques do not take into consideration the effect of the environment, e.g., a Winkler foundation, when tackling boundary conditions, and have to be amended. In this paper as an example we consider an antiplane problem for a thin elastic strip contacting with a relatively compliant Winkler foundation. Refined boundary conditions at an edge loaded by prescribed stresses are established using a properly adjusted Saint-Venant's principle. They appear to be useful for advanced structure modelling including analysis of the static equilibrium under self-equilibrated loading.

## 1. Introduction

In this paper we address the important issue of the formulation of consistent boundary (edge) conditions in the low-dimensional theories for thin elastic structures supported by a Winkler foundation. The latter is known to be a local model for which the response of the environment at a considered point is assumed to be proportional to the deflection occurring at the same point, see original publications (Fuss, 1793; Winkler, 1867; Zimmermann, 1888) along with contemporary ones (Aghalovyan, 2015; Kaplunov, Prikazchikov, & Sultanova, 2018), concerned with mathematical justification of the Winkler hypothesis. It has been widely used in soil- and geo-mechanics, fracture mechanics, contact mechanics, etc., e.g., see Argatov and Mishuris (2015), Barber (2018), Falope, Lanzoni, and Radi (2022), Krasnitckii, Smirnov, and Gutkin (2023), Lou, Wang, Chen, and Zhai (2011), Malikan (2024), Matysiak and Pauk (2003) and Shugailo, Nobili, and Mishuris (2023) and references therein. Recently, the Winkler model has become revitalised in modelling of micro and nano structures, where similar approximations prove to be useful in both local and nonlocal versions (Gholami & Ansari, 2017; Li, Li, Tan, Fan, & Wang, 2024; Stempin, Pawlak, & Sumelka, 2023).

The derivation of consistent edge conditions is arguably the most involved procedure within the asymptotic theories for thin elastic structures. It is remarkable that the vast majority of publications dealing with these theories mainly consider the equations of motion, with only very few ones oriented to the boundary conditions, see Goldenveizer (1994, 1998), Gregory and Wan (1985), Mathúna (1989) and Wilde, Surova, and Sergeeva (2022). The aforementioned procedure relies on the decay of boundary layers characteristic of the original equations in the theory of elasticity, see monographs (Aghalovyan, 2015; Goldenveizer, 1976; Kaplunov, Kossovich, & Nolde, 1998) and references therein. For a semi-infinite elastic strip, see Gregory and Wan (1984), Kaplunov,

* Corresponding author.
*E-mail address:* wim@aber.ac.uk (W. Miszuris).

https://doi.org/10.1016/j.ijengsci.2024.104152
Received 18 July 2024; Received in revised form 18 September 2024; Accepted 18 September 2024
Available online 5 October 2024

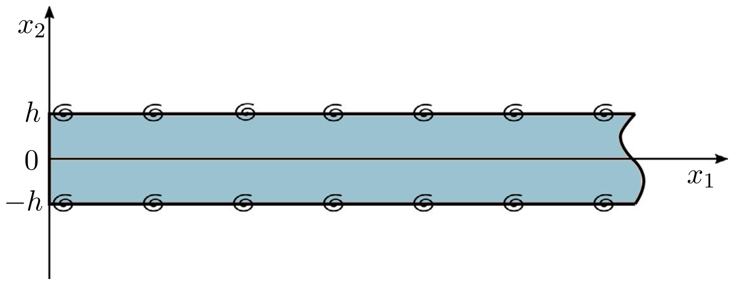


**Fig. 1.** Semi-infinite strip supported by a Winkler-type foundation along two sides.

Prikazchikova, and Alkinidri (2021) and Gusein-Zade (1965), the related decay conditions are apparently the best illustration of the classical Saint-Venant's principle (Love, 2013). They state that for edge in-plane or out-of-plane static loading all stress resultants as well as the longitudinal stress couple have to be equal to zero in order to ensure the stress field to be localised over the vicinity of order of the strip thickness. For arbitrary geometry, the decay conditions for a semi-strip have to be subject to perturbation in the small geometric parameter typical of thin structures in order to evaluate plane and antiplane boundary layers, e.g., see Goldenveizer (1976, 1994, 1998). More recent examples related to perturbation of the decay conditions for an elastic semi-strip involve low-frequency dynamics and high contrast layered composites, see Babenkova and Kaplunov (2004) and Prikazchikova (2022), respectively. We also note that calculation of boundary layers, especially in nonlinear setting, usually relies on extensive direct numerical techniques, see Mishuris, Miszuris, and Öchsner (2007a, 2007b), Mishuris and Öchsner (2005), Mishuris et al. (2005), Miszuris and Öchsner (2013) and Sonato, Piccolroaz, Miszuris, and Mishuris (2015).

All the existing examples of decay conditions consider a semi-infinite elastic strip with traction-free sides, modelled by Neumann-type boundary conditions. At the same time, numerous applications inspire analysis of more general conditions along the sides, taking into account a contact with environment, including the above mentioned Winkler elastic foundation. Its presence leads to mixed Robin boundary conditions along the sides. As a result, numerous ad-hoc formulations for thin structures resting on Winkler foundations, e.g., see Frỳba (2013) and Kaplunov, Prikazchikov, Rogerson, and Lashab (2014), have to be ideally revisited returning back to the original 3D framework based on the aforementioned mixed conditions. This issue has been recently addressed for the equations of motion governing bending of elastically supported beams and plates in Erbaş, Kaplunov, and Elishakoff (2022) and Erbaş, Kaplunov, and Kiliç (2022a), see also Erbaş, Kaplunov, Nobili, and Kılıç (2018), assuming that the structural stiffness is much greater than that of the foundation. However, the effect of a Winkler foundation on the boundary conditions along structure edges has not yet been studied.

In this paper we are aiming at extending the canonical Saint-Venant's principle to a semi-infinite strip interacting with a relatively soft Winkler foundation. Similarly to Kaplunov et al. (2021) and Prikazchikova (2022), a perturbation approach, using a small parameter corresponding to the relative stiffness of the foundation is developed. For the sake of simplicity, we restrict ourselves to a scalar antiplane problem. Both one- and two-sided foundations are considered.

In the paper the leading order decay condition corresponding to self-equilibrated shear edge stress is corrected by incorporating higher order terms taking into account the effect of the foundation. Explicit three-term asymptotic expansions are derived. They are implemented to formulate the consistent higher order boundary conditions for 1D equilibrium equations governing long-scale shear deformation of the semi-strip. The derivation of these equations is more straightforward and can be found in Appendix. It readily adapts the asymptotic procedure exploited in the theory for plates and shells since long ago, e.g., see Goldenveizer (1976), Goldenveizer, Kaplunov, and Nolde (1993) and Kaplunov, Erbaş, and Ege (2022), as well as more recent papers (Erbaş et al., 2022, 2022a) taking into account the presence of the Winkler foundation. The obtained results are useful for assessment of the traditional approach ignoring the effect of the foundation on the boundary conditions. In particular, it appears that the established boundary conditions incorporating this effect are suitable for evaluating the asymptotic interior solution due to a self-equilibrated edge loading.

We also remark that the problem in antiplane elasticity studied in the paper is governed by the same Laplace equation with Robin boundary conditions as its counterpart in the theory of heat or mass transfer. In those cases, the classical Fourier or Darcy laws support a similar effect as the contact with a Winkler foundation, see for example Marušić-Paloka and Pažanin (2022).

## 2. Two-sided Winkler foundation

### 2.1. Statement of the problem

Consider antiplane shear of a semi-infinite elastic strip ($0 \le x_1 < +\infty$, $-h \le x_2 \le h$) interacting with a Winkler-type foundation along its horizontal sides, see Fig. 1. The strip equilibrium is given by

$$\frac{\partial \sigma_{31}}{\partial x_1} + \frac{\partial \sigma_{32}}{\partial x_2} = 0, \tag{1}$$

with

$$\sigma_{3i} = \mu \frac{\partial u}{\partial x_i}, \qquad i = 1, 2, \tag{2}$$

where $\sigma_{3i} = \sigma_{3i}(x_1, x_2)$ are shear stresses, $\mu$ is a Lamé parameter and $u = u(x_1, x_2)$ is an out-of-plane displacement.

The mixed boundary conditions modelling the strip contact with the foundation are taken as

$$\sigma_{32} = \mp ku \qquad \text{at} \quad x_2 = \pm h, \tag{3}$$

where $k$ denotes the stiffness of the foundation. We also assume that the shearing stress $p(x_2)$ is prescribed at the strip edge, i.e.

$$\sigma_{31} = p(x_2) \qquad \text{at} \quad x_1 = 0. \tag{4}$$

### 2.2. Classical low-dimensional model and associated small parameters

In engineering applications the formulated 2D problem (1)–(4) is often approximated by 1D problem, e.g., see Goldenveizer (2014) dealing with more general setup by averaging the displacement and stress over the strip cross-section. In this case, the average displacement $v(x_1)$ and the stress resultant $S(x_1)$ are given by

$$v(x_1) = \frac{1}{2h}\int_{-h}^{h} u(x_1, x_2)dx_2, \quad S(x_1) = \int_{-h}^{h} \sigma_{31}(x_1, x_2)dx_2. \tag{5}$$

As it follows from (2), these quantities are related by

$$S = 2\mu h \frac{dv}{dx_1}, \tag{6}$$

while Eq. (1) after integrating over $x_2$ and taking into account the boundary conditions (3) can be written as

$$\frac{dS}{dx_1} - k\Big(u(x_1, h) + u(x_1, -h)\Big) = 0. \tag{7}$$

The latter, using the trapezoidal rule, see Atkinson (1991), transforms to

$$\frac{dS}{dx_1} - 2kv = kh^2 R_h, \tag{8}$$

where

$$R_h(x_1) = \frac{2}{3}\frac{\partial^2 u}{\partial x_2^2}(x_1, \gamma(x_1)), \quad \gamma \in (-h, h),$$

with some unknown function $\gamma(x_1)$. Thus, the homogeneous equation corresponding to (8) has the truncation error of $O(h^2/L^2)$, where $L$ is a typical length scale.

As a result of this trivial consideration, we may also arrive by differentiating (8) at a limiting 1D problem given by the second-order equation

$$\frac{d^2S}{dx_1^2} - \frac{k}{\mu h}S = kh^2\frac{dR_h}{dx_1}, \tag{9}$$

or at leading order

$$\frac{d^2S}{dx_1^2} - \frac{k}{\mu h}S = 0. \tag{10}$$

The boundary condition to this equation at the edge $x_1 = 0$ takes the form

$$S(0) = \int_{-h}^{h} p(x_2)dx_2. \tag{11}$$

This condition follows from its 2D counterpart (4) due to the classical Saint-Venant's principle, generally assuming traction free but not elastically supported semi-infinite sides of the strip; for the former, $k = 0$ in the formulae above. In this case, 1D formulation in terms of the shear stress resultant $S$, given by the equilibrium equation

$$\frac{dS}{dx_1} = 0, \tag{12}$$

following from (8), subject to boundary condition (11), is the exact consequence of the initial 2D setup.

However, at $k > 0$, the presence of the remainder $R_h$ in the right-hand side of Eq. (8) necessitates special consideration. It is rather obvious that $R_h$ is small over the interior of the semi-strip ($x_1 \gg h$) when $h \ll L$, while near the edge ($x_1 \sim h$), when $h \sim L$, the adapted above trapezoidal approximation is not robust.

It might be expected that the restoration of the 2D solution of the original problem (1)–(4) from a 1D formulation assumes a similar asymptotic insight as for a strip with free sides.

At the same time, the traditional asymptotic scheme underlying dimension reduction in mechanics of thin elastic structures, e.g., see Goldenveizer (1976) and Kaplunov et al. (1998), usually assumes Neumann-type boundary conditions along the sides. It ideally has to be revisited for the structures interacting with a Winkler foundation, see recent papers (Erbaş et al., 2022, 2022a) considering the equations of motion only. The effect of a Winkler foundation on the boundary conditions including the corrections to the canonical formulation of the Saint-Venant's principle has not been yet investigated.

Below we perform an accurate asymptotic analysis of the simplest 2D setup given by (1)–(4) in order to justify and refine the 1D model (10)–(11). The main focus is on the dimension reduction of the boundary condition (4) taking into consideration the variation of the prescribed edge stress $p(x_2)$ across the thickness of the strip.

As a preliminary observation we remark that for a self-equilibrated $p(x_2)$ the formula (11) corresponds to a homogeneous boundary condition justified for traction free sides ($k = 0$). However, it is clear intuitively that it should not be the case in presence of a foundation ($k > 0$), see also papers (Kaplunov et al., 2021; Prikazchikova, 2022) dealing with perturbations of static decay conditions for a semi-strip with traction free sides.

As a small parameter we adapt a properly dimensionalised ratio of the Winkler foundation stiffness and the strip shear modulus given by

$$\varepsilon = \frac{kh}{\mu} \ll 1. \tag{13}$$

This parameter is similar to that in papers (Erbaş et al., 2022a, 2018) supporting thin plate bending in presence of Winkler foundation. We also know that the formula (13) rewritten for $\sqrt{\varepsilon}$ can be presented as

$$\sqrt{\varepsilon} = \frac{h}{L} \ll 1, \tag{14}$$

where the length scale is given by

$$L = \sqrt{\frac{h\mu}{k}}. \tag{15}$$

If (13) or (14) are violated, then the strip is not thin enough or the Winkler foundation is not soft enough to allow the dimension reduction.

### *2.3. Scaling for the original 2D antiplane problem*

In what follows we use the dimensionless variables

$$\xi = \frac{x_1}{h} \quad \text{and} \quad \zeta = \frac{x_2}{h}, \tag{16}$$

as well as the dimensionless quantities

$$\sigma_{3i}^* = \frac{\sigma_{3i}}{\mu}, \quad p^* = \frac{p}{\mu} \quad \text{and} \quad u^* = \frac{u}{h}. \tag{17}$$

Relations (1)–(4) then become

$$\frac{\partial \sigma_{31}^*}{\partial \xi} + \frac{\partial \sigma_{32}^*}{\partial \zeta} = 0, \tag{18}$$

and

$$\sigma_{31}^* = \frac{\partial u^*}{\partial \xi}, \qquad \sigma_{32}^* = \frac{\partial u^*}{\partial \zeta}, \tag{19}$$

subject to

$$\sigma_{32}^* = \mp \varepsilon u^* \qquad \text{at} \quad \zeta = \pm 1, \tag{20}$$

and

$$\sigma_{31}^* = p^*(\zeta) \qquad \text{at} \quad \xi = 0. \tag{21}$$

In terms of dimensionless displacements the problem can be rewritten as

$$\frac{\partial^2 u^*}{\partial \xi^2} + \frac{\partial^2 u^*}{\partial \zeta^2} = 0, \tag{22}$$

subject to

$$\frac{\partial u^*}{\partial \zeta} = \mp \varepsilon u^* \qquad \text{at} \quad \zeta = \pm 1, \tag{23}$$

and

$$\frac{\partial u^*}{\partial \xi} = p^*(\zeta) \qquad \text{at} \quad \xi = 0. \tag{24}$$

### 2.4. Decay conditions and a boundary layer

We begin with the asymptotic generalisation of the Saint-Venant's principle corresponding to the mixed boundary conditions along the sides, see (20) or (23). In what follows we derive corrections to the well-known decay conditions for traction free sides ($\varepsilon = 0$), e.g., see Gusein-Zade (1965), dictating the self-equilibrium of the prescribed load $p(x_2)$. In this case we assume

$$\sigma_{31}^* \to 0 \quad \text{and} \quad u^* \to 0 \qquad \text{as} \quad \xi \to \infty. \tag{25}$$

First, integrating Eq. (18) over the domain $0 \le \xi < \infty$, $-1 \le \zeta \le 1$, we obtain

$$\int_{-1}^{1} p^* d\zeta + \varepsilon \int_0^\infty \left( u^*\Big|_{\zeta=1} + u^*\Big|_{\zeta=-1} \right) d\xi = 0. \tag{26}$$

As might be expected, the last formula at $\varepsilon = 0$ gives the aforementioned decay condition expressing the Saint-Venant's principle. Now, expand $p^*$ and $u^*$ in asymptotic series as

$$\begin{aligned} p^* &= p_0^* + \varepsilon p_1^* + \varepsilon^2 p_2^* + \cdots, \\ u^* &= u_0^* + \varepsilon u_1^* + \varepsilon^2 u_2^* + \cdots, \end{aligned} \tag{27}$$

where $p_0^*(\zeta)$ is a self-equilibrated load satisfying

$$\int_{-1}^{1} p_0^* d\zeta = 0, \tag{28}$$

while $p_i^*$, $i = 1, 2, \ldots$, are, in general, non self-equilibrated ones. Without loss of generality, the latter may be assumed to be constants. Indeed if $p_i^*(\zeta)$ is not a constant, it can be represented as a sum $p_{i0}^*(\zeta)$ and $p_{ic}^*$, where the former is self-equilibrated (and thus is accounted for by $p_0^*(\zeta)$), while the latter is a constant.

*Leading order approximation*

Taking into account (28), $p_0^*$ can be written as

$$p_0^*(\zeta) = \sum_{n=1}^{\infty} A_n \cos(\alpha_n \zeta) + \sum_{n=1}^{\infty} B_n \sin(\beta_n \zeta), \tag{29}$$

where

$$\alpha_n = n\pi, \qquad \beta_n = \frac{(2n-1)\pi}{2}. \tag{30}$$

The coefficients in (29) take the form

$$A_n = \int_{-1}^{1} p_0^* \cos(\alpha_n \zeta) d\zeta, \qquad n = 1, 2, \ldots, \tag{31}$$

and

$$B_n = \int_{-1}^{1} p_0^* \sin(\beta_n \zeta) d\zeta, \qquad n = 1, 2, \ldots \tag{32}$$

Also, we have from (22)–(24) and (27)

$$\frac{\partial^2 u_0^*}{\partial \xi^2} + \frac{\partial^2 u_0^*}{\partial \zeta^2} = 0, \tag{33}$$

subject to

$$\frac{\partial u_0^*}{\partial \zeta} = 0 \qquad \text{at} \quad \zeta = \pm 1, \tag{34}$$

and

$$\frac{\partial u_0^*}{\partial \xi} = p_0^* \qquad \text{at} \quad \xi = 0. \tag{35}$$

The solution of the boundary value problem is given by

$$u_0^* = -\sum_{n=1}^{\infty} \frac{A_n}{\alpha_n} e^{-\alpha_n \xi} \cos(\alpha_n \zeta) - \sum_{n=1}^{\infty} \frac{B_n}{\beta_n} e^{-\beta_n \xi} \sin(\beta_n \zeta). \tag{36}$$

*First order approximation*

At next order, we obtain from (26) a formula for the correction to the leading order decay condition (28) in the form

$$\int_{-1}^{1} p_1^* d\zeta + \int_0^\infty \left( u_0^*\Big|_{\zeta=1} + u_0^*\Big|_{\zeta=-1} \right) d\xi = 0. \tag{37}$$

On inserting (36) into this condition we obtain

$$p_1^* = \sum_{n=1}^{\infty} \frac{(-1)^n A_n}{\alpha_n^2}. \tag{38}$$

The constant $p_1^*$ can also be expressed as

$$p_1^* = \frac{1}{4}\int_{-1}^{1} p_0^*(\zeta)\left(\zeta^2 - \frac{1}{3}\right) d\zeta. \tag{39}$$

At this order we can also determine $u_1^*$ from the following boundary value problem

$$\frac{\partial^2 u_1^*}{\partial \xi^2} + \frac{\partial^2 u_1^*}{\partial \zeta^2} = 0, \tag{40}$$

subject to

$$\frac{\partial u_1^*}{\partial \zeta} = \mp u_0^* \qquad \text{at} \quad \zeta = \pm 1, \tag{41}$$

and

$$\frac{\partial u_1^*}{\partial \xi} = p_1^* \qquad \text{at} \quad \xi = 0. \tag{42}$$

This problem, in contrast to the leading order one, involves non-homogeneous boundary conditions along the sides, cf. (34) and (41).

Let us present $u_1^*$ in the series form as

$$\begin{aligned} u_1^* = \sum_{n=1}^{\infty} \big\{ & E_n \cos(\alpha_n\zeta)e^{-\alpha_n\xi} + F_n \sin(\beta_n\zeta)e^{-\beta_n\xi} + G_n\zeta \sin(\alpha_n\zeta)e^{-\alpha_n\xi} \\ & + H_n\zeta \cos(\beta_n\zeta)e^{-\beta_n\xi} + I_n\xi \cos(\alpha_n\zeta)e^{-\alpha_n\xi} + K_n\xi \sin(\beta_n\zeta)e^{-\beta_n\xi} \big\}, \end{aligned} \tag{43}$$

where $E_n, F_n, G_n, H_n, I_n$ and $K_n$ are sought for constants. Four of them can be found by substituting (43) into (40) and (41). They are

$$G_n = I_n = \frac{A_n}{\alpha_n^2}, \qquad H_n = -K_n = -\frac{B_n}{\beta_n^2}. \tag{44}$$

Remaining constants $E_n$ and $F_n$ follow from (42), which becomes

$$\sum_{n=1}^{\infty} \left\{ (I_n - \alpha_n E_n)\cos(\alpha_n\zeta) + (K_n - \beta_n F_n)\sin(\beta_n\zeta) - \alpha_n G_n \zeta \sin(\alpha_n\zeta) - \beta_n H_n \zeta \cos(\beta_n\zeta) \right\} = p_1^*. \tag{45}$$

Next, we expand $\zeta \sin(\alpha_n\zeta)$ and $\zeta \cos(\beta_n\zeta)$ into series having

$$\zeta \sin(\alpha_n\zeta) = \frac{S_0^{(n)}}{2} + \sum_{k=1}^{\infty} S_k^{(n)} \cos(\alpha_k\zeta), \quad \zeta \cos(\beta_n\zeta) = \sum_{k=1}^{\infty} P_k^{(n)} \sin(\beta_k\zeta), \tag{46}$$

where

$$S_0^{(n)} = -\frac{2(-1)^n}{\alpha_n} = -\frac{2(-1)^n}{\pi n}, \quad S_k^{(n)} = \int_{-1}^{1} \zeta \sin(\alpha_n\zeta)\cos(\alpha_k\zeta) d\zeta, \tag{47}$$

and

$$P_k^{(n)} = \int_{-1}^{1} \zeta \cos(\beta_n\zeta)\sin(\beta_k\zeta) d\zeta. \tag{48}$$

The integrals in (47) and (48) can be evaluated as

$$S_k^{(n)} = \begin{cases} -\dfrac{1}{2\alpha_k} = -\dfrac{1}{2\pi k}, & \text{if } k = n, \\ \dfrac{2(-1)^{k+n}\alpha_n}{\alpha_k^2 - \alpha_n^2} = \dfrac{2(-1)^{k+n} n}{\pi(k^2 - n^2)}, & \text{if } k \neq n, \end{cases} \tag{49}$$

and

$$P_k^{(n)} = \begin{cases} \dfrac{1}{2\beta_k} = \dfrac{1}{\pi(2k-1)}, & \text{if } k = n, \\ -\dfrac{2(-1)^{k+n}\beta_n}{\beta_k^2 - \beta_n^2} = -\dfrac{(-1)^{k+n}(2n-1)}{\pi(k+n-1)(k-n)}, & \text{if } k \neq n. \end{cases} \tag{50}$$

Then substituting expansions (46) back into (45), we finally derive

$$E_n = \frac{1}{\alpha_n}\left(\frac{A_n}{\alpha_n^2} - \sum_{k=1}^{\infty} \frac{A_k}{\alpha_k} S_n^{(k)}\right), \qquad F_n = \frac{1}{\beta_n}\left(\frac{B_n}{\beta_n^2} + \sum_{k=1}^{\infty} \frac{B_k}{\beta_k} P_n^{(k)}\right). \tag{51}$$

Thus, the term $u_1^*$ has now been fully defined.

*Second order approximation*

At second order, we have from the condition (26)

$$\int_{-1}^{1} p_2^* d\zeta + \int_0^\infty \left( u_1^*\Big|_{\zeta=1} + u_1^*\Big|_{\zeta=-1} \right) d\xi = 0. \tag{52}$$

Substituting $u_1^*$, found at the previous step, see (43), we obtain for the sought for constant $p_2^*$

$$p_2^* = -\sum_{n=1}^{\infty} \frac{(-1)^n}{\alpha_n^2} \left( \frac{2A_n}{\alpha_n^2} - \sum_{k=1}^{\infty} \frac{A_k}{\alpha_k} S_n^{(k)} \right). \tag{53}$$

This expression can also be rewritten as

$$p_2^* = \frac{1}{48} \int_{-1}^{1} p_0^*(\zeta) \left( -\zeta^4 - 2\zeta^2 + \frac{13}{15} \right) d\zeta. \tag{54}$$

Finally, combining the decay conditions obtained above at zero, first and second orders, by adding Eq. (28), (37), and (52), multiplied by $\varepsilon^n$ with $n = 0, 1, 2$, respectively, and using the asymptotic expansions for $p^*$ in (27), we obtain

$$\int_{-1}^{1} p^*(\zeta) \left\{ 1 - \frac{\varepsilon}{2} \left( \zeta^2 - \frac{1}{3} \right) + \frac{\varepsilon^2}{24} \left( \zeta^4 + 2\zeta^2 - \frac{13}{15} \right) \right\} d\zeta = 0, \tag{55}$$

where $O(\varepsilon^3)$ terms have been neglected.

### 2.5. Derivation of boundary conditions for 1D equilibrium equations

Let us apply decay condition (55) for derivation of the boundary conditions to the 1D Eq. (A.13) for the out-of-plane displacement of the mid-strip, derived in Appendix. Consider the edge of a semi-infinite strip $x_1 = 0$ subject to an arbitrary shearing force $q(x_2)$. In this case, the 2D boundary condition, see the original formulation (21) in Section 2.3, can be written as

$$\sigma_{31}^*|_{\xi=0} = q^*(\zeta), \tag{56}$$

where $\sigma_{31}^*$ is given by (19) and $q^* = q/\mu$. Generally, $q^*$ may not obey (55).

As usual, e.g., see Kaplunov et al. (2021) and Wan (2000) and references therein, we consider the discrepancy between prescribed arbitrary stress $q^*$ and the interior stress $q_{int}^*$, given by (A.14), which is polynomial in the transverse variable $\zeta$. This discrepancy has to satisfy the decay condition (55) in order to form a boundary layer, localised in a small $h$-vicinity of the edge. Therefore, substituting $p^* = q^* - q_{int}^*\Big|_{\xi=0}$ into (55), we arrive at the sought for boundary condition for the solution over the interior. It is

$$\frac{dU^*}{d\xi}\Big|_{\xi=0} = \frac{1}{2} \int_{-1}^{1} q^*(\zeta) \left\{ 1 - \frac{\varepsilon}{2} \left( \zeta^2 - \frac{2}{3} \right) + \frac{\varepsilon^2}{24} \left( \zeta^4 - \frac{8}{5} \right) \right\} d\zeta, \tag{57}$$

where dimensionless mid-plane displacement $U^*$ is defined by (A.13) in Appendix. Obviously, only even functions $q^*(\zeta)$ would result in inhomogeneous boundary conditions (57). As an illustration, we specify the boundary condition (57) for several external loads

(i) $q^* = 1$

$$\frac{dU^*}{d\xi}\Big|_{\xi=0} = 1 + \frac{1}{6}\varepsilon - \frac{7}{120}\varepsilon^2, \tag{58}$$

(ii) $q^* = \zeta^2$

$$\frac{dU^*}{d\xi}\Big|_{\xi=0} = \frac{1}{3} + \frac{1}{90}\varepsilon - \frac{41}{2520}\varepsilon^2, \tag{59}$$

(iii) $q^* = 1 - 3\zeta^2 + \delta$, where $\delta$ is a real constant

$$\frac{dU^*}{d\xi}\Big|_{\xi=0} = \delta + \varepsilon \left( \frac{2}{15} + \frac{1}{6}\delta \right) - \varepsilon^2 \left( \frac{1}{105} + \frac{7}{120}\delta \right). \tag{60}$$

As might be expected, the presented formulae, including the last one, corresponding to a self-equilibrated stress $q^*$ when $\delta = 0$, incorporate the derived corrections to the Saint-Venant's principle.

Numerical results illustrating formula (60) are presented in Figs. 2 and 3. The relative error, $e_r$, of the traditional boundary condition

$$\frac{dU^*}{d\xi}\Big|_{\xi=0} = \delta, \tag{61}$$

with respect to the asymptotically refined condition (60) is calculated by

$$e_r = \left| 1 - \frac{\delta}{\delta + \frac{2}{15}\varepsilon + \frac{1}{6}\delta\varepsilon - \varepsilon^2 \left( \frac{1}{105} + \frac{7}{120}\delta \right)} \right| \times 100\%. \tag{62}$$

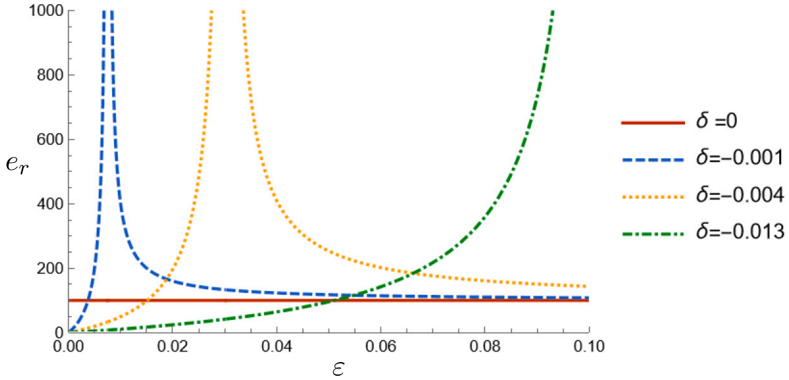


**Fig. 2.** The relative error of the canonical boundary condition ($\varepsilon = 0$ in (60)) versus to the refined one (60) for $\delta \leqslant 0$.

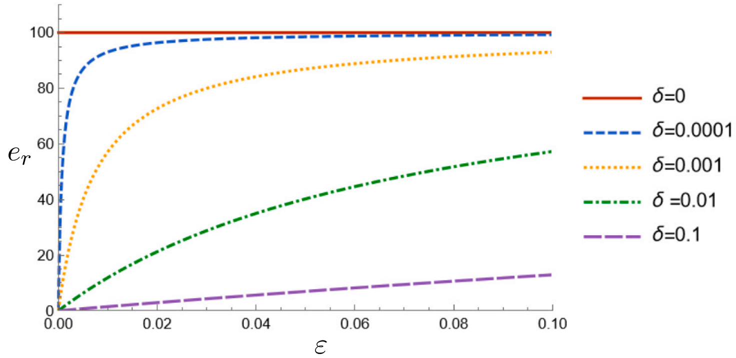


**Fig. 3.** The relative error of the canonical boundary condition ($\varepsilon = 0$ in (60)) versus to the refined one (60) for $\delta \geqslant 0$.

At $\delta = 0$ the last expression gives $e_r = 100\%$, whereas at $\delta \ll \varepsilon \ll 1$ $e_r \approx 100\%$. It is worth noting that at $\delta/\varepsilon = -2/15$ the denominator in the formula (62) degenerates at leading order resulting in $e_r \gg 100\%$, see Fig. 2, where $\delta/\varepsilon = -2/15$ at $\varepsilon = 0.0075$, $\varepsilon = 0.03$ and $\varepsilon = 0.1$ for $\delta = -0.001$, $\delta = -0.004$ and $\delta = -1/75 \approx -0.013$, respectively. Physically it means that non self-equilibrated loads at $\delta < 0$ may not induce an inhomogeneity of the same magnitude in boundary condition (60). This observation does not hold true for $\delta > 0$, when $e_r < 100\%$, see Fig. 3.

## 3. One-sided Winkler foundation

### *3.1. The boundary value problem*

Below we extend the problem considered in the previous section to a more technical setup of a semi-infinite elastic strip supported by a Winkler foundation along the side $x_2 = -h$ only, see Fig. 4. The problem formulation is the same as that for a two-sided foundation, see (1)–(4), except the boundary conditions (3) along the sides now taking the form

$$\sigma_{32} = ku \quad \text{at} \quad x_2 = -h, \qquad \sigma_{32} = 0 \quad \text{at} \quad x_2 = h. \tag{63}$$

For one-sided setup the 1D engineering model is also similar to that presented in Section 2 and is given by

$$\frac{d^2 S}{d x_1^2} - \frac{k}{2\mu h} S = 0, \quad S(0) = \int_{-h}^{h} p(x_2) d x_2. \tag{64}$$

As might be expected, the coefficient at the second term in the first Eq. (64) is twice less than its counterpart in Eq. (10).

In what follows, as before, the goal is to justify and refine the elementary engineering framework.

In the dimensionless form, now we have instead of (20)

$$\begin{aligned} \sigma_{32}^* &= \frac{\partial u^*}{\partial \zeta} = \varepsilon u^* \quad \text{at} \quad \zeta = -1, \\ \sigma_{32}^* &= \frac{\partial u^*}{\partial \zeta} = 0 \quad \text{at} \quad \zeta = 1. \end{aligned} \tag{65}$$

Other relevant formulae, including (18) and (21), presented in Section 2, stay the same.

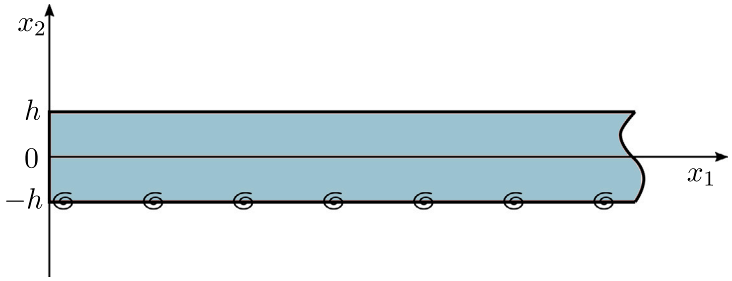


**Fig. 4.** Semi-infinite strip supported by a Winkler-type foundation along one side.

### 3.2. Decay conditions

Integrating Eq. (18) over the domain and using conditions (21) and (65) we now obtain

$$\int_{-1}^{1} p^* d\zeta + \varepsilon \int_{0}^{\infty} u^*\Big|_{\zeta=-1} d\xi = 0. \tag{66}$$

As might be expected, the leading order solution is identical to that in Section 2.4 for a two-sided Winkler foundation, including formulae (29) and (36) for $p_0^*$ and $u_0^*$, respectively.

At first order we obtain from (66)

$$\int_{-1}^{1} p_1^* d\zeta + \int_{0}^{\infty} u_0^*\Big|_{\zeta=-1} d\xi = 0. \tag{67}$$

By substituting (36) into (67) we get

$$p_1^* = \frac{1}{2}\sum_{n=1}^{\infty}(-1)^n\left(\frac{A_n}{\alpha_n^2}+\frac{B_n}{\beta_n^2}\right) = \frac{1}{8}\int_{-1}^{1} p_0^*(\zeta)\left(\zeta^2-2\zeta-\frac{1}{3}\right)d\zeta, \tag{68}$$

where $\alpha_n$, $\beta_n$, $A_n$ and $B_n$ are defined in (30)–(32).

The first order boundary value problem for the displacement becomes

$$\frac{\partial^2 u_1^*}{\partial \xi^2}+\frac{\partial^2 u_1^*}{\partial \zeta^2} = 0, \tag{69}$$

subject to

$$\frac{\partial u_1^*}{\partial \zeta} = u_0^* \quad \text{at} \quad \zeta=-1, \qquad \frac{\partial u_1^*}{\partial \zeta} = 0 \quad \text{at} \quad \zeta = 1, \tag{70}$$

and

$$\frac{\partial u_1^*}{\partial \xi} = p_1^* \qquad \text{at} \quad \xi = 0. \tag{71}$$

Taking $u_1^*$ in the form

$$\begin{aligned} u_1^* = \sum_{n=1}^{\infty}\Big\{&\tilde{E}_n\cos(\alpha_n\zeta)e^{-\alpha_n\xi}+\tilde{F}_n\sin(\beta_n\zeta)e^{-\beta_n\xi}+\tilde{G}_n\zeta\sin(\alpha_n\zeta)e^{-\alpha_n\xi}+\tilde{H}_n\zeta\cos(\beta_n\zeta)e^{-\beta_n\xi}\\ &+\tilde{I}_n\xi\cos(\alpha_n\zeta)e^{-\alpha_n\xi}+\tilde{K}_n\xi\sin(\beta_n\zeta)e^{-\beta_n\xi}+\tilde{L}_n\sin(\alpha_n\zeta)e^{-\alpha_n\xi}+\tilde{M}_n\cos(\beta_n\zeta)e^{-\beta_n\xi}\Big\}, \end{aligned} \tag{72}$$

and using Eqs. (69)–(70) we determine six out of eight unknown constants, namely

$$\tilde{G}_n = \tilde{I}_n = -\tilde{L}_n = \frac{A_n}{2\alpha_n^2}, \qquad \tilde{K}_n = \tilde{M}_n = -\tilde{H}_n = \frac{B_n}{2\beta_n^2}. \tag{73}$$

Then, the boundary condition (71) gives

$$\begin{aligned} \sum_{n=1}^{\infty}\Big\{&(\tilde{I}_n-\alpha_n\tilde{E}_n)\cos(\alpha_n\zeta)+(\tilde{K}_n-\beta_n\tilde{F}_n)\sin(\beta_n\zeta)-\alpha_n\tilde{G}_n\zeta\sin(\alpha_n\zeta)\\ &-\beta_n\tilde{H}_n\zeta\cos(\beta_n\zeta)-\alpha_n\tilde{L}_n\sin(\alpha_n\zeta)-\beta_n\tilde{M}_n\cos(\beta_n\zeta)\Big\} = p_1^*. \end{aligned} \tag{74}$$

Next, we expand $\sin(\alpha_n\zeta)$ and $\cos(\beta_n\zeta)$ into series

$$\sin(\alpha_n\zeta) = \sum_{k=1}^{\infty} R_k^{(n)}\sin(\beta_k\zeta), \qquad \cos(\beta_n\zeta) = \frac{T_0^{(n)}}{2}+\sum_{k=1}^{\infty} T_k^{(n)}\cos(\alpha_k\zeta), \tag{75}$$

where

$$
\begin{aligned}
T_0^{(n)} &= \frac{2(-1)^{n+1}}{\beta_n} = \frac{4(-1)^{n+1}}{\pi(2n-1)},\\
T_k^{(n)} &= -\frac{2(-1)^{n+k}\beta_n}{\beta_n^2-\alpha_k^2} = -\frac{4(-1)^{n+k}(2n-1)}{\pi\left((2n-1)^2-4k^2\right)},\\
R_k^{(n)} &= \frac{2(-1)^{n+k}\alpha_n}{\alpha_n^2-\beta_k^2} = \frac{8(-1)^{n+k}n}{\pi\left(4n^2-(2k-1)^2\right)}.
\end{aligned}
\tag{76}
$$

Using expansions (46) and (75) as well as relation (68), Eq. (74) can be transformed to

$$
\begin{aligned}
\sum_{n=1}^{\infty}\Bigg\{&\left(\tilde{I}_n-\alpha_n\tilde{E}_n-\sum_{k=1}^{\infty}\alpha_k\tilde{G}_kS_n^{(k)}-\sum_{k=1}^{\infty}\beta_k\tilde{M}_kT_n^{(k)}\right)\cos(\alpha_n\zeta)\\
&+\left(\tilde{K}_n-\beta_n\tilde{F}_n-\sum_{k=1}^{\infty}\alpha_k\tilde{L}_kR_n^{(k)}-\sum_{k=1}^{\infty}\beta_k\tilde{H}_kP_n^{(k)}\right)\sin(\beta_n\zeta)\Bigg\}=0.
\end{aligned}
\tag{77}
$$

Finally, we derive

$$
\begin{aligned}
\tilde{E}_n &= \frac{1}{2\alpha_n}\left(\frac{A_n}{\alpha_n^2}-\sum_{k=1}^{\infty}\frac{A_k}{\alpha_k}S_n^{(k)}-\sum_{k=1}^{\infty}\frac{B_k}{\beta_k}T_n^{(k)}\right),\\
\tilde{F}_n &= \frac{1}{2\beta_n}\left(\frac{B_n}{\beta_n^2}+\sum_{k=1}^{\infty}\frac{A_k}{\alpha_k}R_n^{(k)}+\sum_{k=1}^{\infty}\frac{B_k}{\beta_k}P_n^{(k)}\right).
\end{aligned}
\tag{78}
$$

At the second order, Eq. (66) gives a similar to (52) condition

$$
\int_{-1}^{1}p_2^*d\zeta+\int_0^{\infty}u_1^*\Big|_{\zeta=-1}d\xi=0. \tag{79}
$$

Then, we arrive at

$$
p_2^* = -\frac{1}{4}\sum_{n=1}^{\infty}(-1)^n\left\{\frac{1}{\alpha_n^2}\left(\frac{2A_n}{\alpha_n^2}-\sum_{k=1}^{\infty}\frac{A_k}{\alpha_k}S_n^{(k)}-\sum_{k=1}^{\infty}\frac{B_k}{\beta_k}T_n^{(k)}\right)+\frac{1}{\beta_n^2}\left(\frac{2B_n}{\beta_n^2}+\sum_{k=1}^{\infty}\frac{A_k}{\alpha_k}R_n^{(k)}+\sum_{k=1}^{\infty}\frac{B_k}{\beta_k}P_n^{(k)}\right)\right\}, \tag{80}
$$

which can be rewritten in the form

$$
p_2^* = \frac{1}{192}\int_{-1}^{1}p_0^*(\zeta)\left(-\zeta^4+4\zeta^3-14\zeta^2+20\zeta+\frac{73}{15}\right)d\zeta. \tag{81}
$$

Finally, similarly to the consideration in Section 2, we obtain from (28), (67), and (79) the sought for asymptotic decay condition for a one-sided Winkler foundation. It is given by

$$
\int_{-1}^{1}p^*(\zeta)\left\{1-\frac{\varepsilon}{4}\left(\zeta^2-2\zeta-\frac{1}{3}\right)+\frac{\varepsilon^2}{96}\left(\zeta^4-4\zeta^3+14\zeta^2-20\zeta-\frac{73}{15}\right)\right\}d\zeta=0. \tag{82}
$$

### 3.3. Boundary conditions for 1D equilibrium equations

In this case the interior stress can be found in the form

$$
q_{int}^* = \sigma_{31}^* = \frac{dU^*}{d\xi}\left\{1+\varepsilon\left(\frac{1}{2}\zeta-\frac{1}{4}\zeta^2\right)+\varepsilon^2\left(-\frac{1}{4}\zeta+\frac{1}{6}\zeta^2-\frac{1}{24}\zeta^3+\frac{1}{96}\zeta^4\right)\right\}, \tag{83}
$$

see corresponding Eq. (A.23) from Appendix. Next, similarly to the two-sided case, substituting the difference $p^* = q^* - q_{int}^*\Big|_{\xi=0}$ into decay condition (82), we obtain the boundary condition

$$
\frac{dU^*}{d\xi}\Big|_{\xi=0} = \frac{1}{2}\int_{-1}^{1}q^*(\zeta)\left\{1-\frac{\varepsilon}{4}\left(\zeta^2-2\zeta-\frac{2}{3}\right)+\frac{\varepsilon^2}{96}\left(\zeta^4-4\zeta^3+12\zeta^2-16\zeta-\frac{88}{5}\right)\right\}d\zeta, \tag{84}
$$

where the mid-plane displacement $U^*$ is defined by (A.22) and $q^*$ introduced in (56).

Below, boundary condition (84) is evaluated for several external loads

(i) $q^* = 1$

$$
\frac{dU^*}{d\xi}\Big|_{\xi=0} = 1+\frac{1}{12}\varepsilon-\frac{67}{480}\varepsilon^2, \tag{85}
$$

(ii) $q^* = \zeta^2$

$$
\frac{dU^*}{d\xi}\Big|_{\xi=0} = \frac{1}{3}+\frac{1}{180}\varepsilon-\frac{349}{10080}\varepsilon^2, \tag{86}
$$

(iii) $q^* = 1 - 3\zeta^2$

$$\frac{dU^*}{d\xi}\Big|_{\xi=0} = \frac{1}{15}\varepsilon - \frac{1}{28}\varepsilon^2, \tag{87}$$

(iv) $q^* = \zeta$

$$\frac{dU^*}{d\xi}\Big|_{\xi=0} = \frac{1}{6}\varepsilon - \frac{23}{360}\varepsilon^2, \tag{88}$$

(v) $q^* = 1 - 3\zeta^2 + \zeta$

$$\frac{dU^*}{d\xi}\Big|_{\xi=0} = \frac{7}{30}\varepsilon - \frac{251}{2520}\varepsilon^2, \tag{89}$$

(vi) $q^* = 1 - 3\zeta^2 - \zeta$

$$\frac{dU^*}{d\xi}\Big|_{\xi=0} = -\frac{1}{10}\varepsilon + \frac{71}{2520}\varepsilon^2. \tag{90}$$

Obviously, due to the violation of symmetry, the corrections in the formulae (85)–(87) are not identical to those in the formulae (58)–(60), obtained for two-sided Winkler foundation. Also, inhomogeneous boundary condition (88) as well as deviation in boundary conditions (89) and (90) are specific for one-sided foundation only. The observations for a nearly self-equilibrated load, see (60) and Figs. 2 and 3 in Section 2.5, are also valid for the boundary condition (84).

## 4. Discussion and conclusions

### 4.1. Refined low-dimensional models

The developed asymptotic framework can be implemented for assessment of the low-dimensional models, see (5)–(11) and (64). To this end we rewrite the average stress and displacement given by (5) in the form

$$v(\xi) = \frac{h}{2}\int_{-1}^{1} u^*(\xi,\zeta)d\zeta, \qquad S(\xi) = \mu h \int_{-1}^{1} \sigma_{31}^*(\xi,\zeta)d\zeta. \tag{91}$$

First, consider a two-sided Winkler foundation. In this case, the equations in (A.14) for the interior of the semi-infinite strip can be transformed to

$$S(\xi) = \mu h\left(2 - \frac{1}{3}\varepsilon + \frac{23}{180}\varepsilon^2\right)\frac{dU^*}{d\xi} \tag{92}$$

and

$$v(\xi) = \frac{h}{2}\left(2 - \frac{1}{3}\varepsilon + \frac{23}{180}\varepsilon^2\right)U^*(\xi), \tag{93}$$

where $U^*$ is defined by (A.13). It can be easily verified that $S$ and $v$ satisfy (6).

Using formulae (92) and (93), boundary condition (57) can be recast in the dimensional form as

$$S(0) = \int_{-h}^{h} q(x_2)\left\{1 - \frac{\varepsilon}{2}\left(\frac{x_2^2}{h^2} - \frac{1}{3}\right) + \frac{\varepsilon^2}{24}\left(\frac{x_2^4}{h^4} + 2\frac{x_2^2}{h^2} - \frac{7}{5}\right)\right\}dx_2. \tag{94}$$

Also, Eq. (A.13) can be presented as

$$\frac{dS(x_1)}{dx_1} - 2kv(x_1) = -\frac{2}{3}k\varepsilon\left(1 - \frac{4}{15}\varepsilon\right)v(x_1), \tag{95}$$

demonstrating that the remainder in the right-hand side of Eq. (8) is

$$R_h = -\frac{2}{3h^2}\varepsilon\left(1 - \frac{4}{15}\varepsilon\right)v(x_1). \tag{96}$$

Thus, we arrive at the asymptotic refinement of the engineering problem (5)–(11) expressed in terms of the averaged stress $S(x_1)$ and displacement $v(x_1)$. The truncation error of the derived approximation is $O(\varepsilon^3)$.

We also remark that for the greater truncation error $O(\varepsilon^2)$ only the $O(\varepsilon)$ term has to be retained in the right-hand side of (95). In this case, $O(\varepsilon^2)$ correction can also be neglected in the formula (94).

It is worth mentioning that the developed approach not only enables to derive low-dimensional models but also to restore the original 2D solutions over the interior of the semi-strip within the chosen accuracy.

Similarly, for one-sided foundation we have from (A.23) for the internal stress

$$S(\xi) = \mu h\left(2 - \frac{1}{6}\varepsilon + \frac{83}{720}\varepsilon^2\right)\frac{dU^*}{d\xi}, \tag{97}$$

whereas the implementation of (84) in terms of original variables results in

$$S(0) = \int_{-h}^{h} q(x_2)\left\{1 - \frac{\varepsilon}{4}\left(\frac{x_2^2}{h^2} - 2\frac{x_2}{h} - \frac{1}{3}\right) + \frac{\varepsilon^2}{96}\left(\frac{x_2^4}{h^4} - 4\frac{x_2^3}{h^3} + 14\frac{x_2^2}{h^2} - 20\frac{x_2}{h} - \frac{67}{5}\right)\right\}dx_2. \tag{98}$$

In this case, we also obtain from (A.22)

$$\frac{dS(x_1)}{dx_1} - kv(x_1) = -\frac{2}{3}k\varepsilon\left(1 - \frac{8}{15}\varepsilon\right)v(x_1). \tag{99}$$

*4.2. Higher order decay conditions*

The derivation of the asymptotic decay conditions (55) and (82) is an independent important result of the paper. In original variables they become

$$\int_{-h}^{h} p(x_2)w_\varepsilon(x_2)dx_2 = 0, \tag{100}$$

where

$$w_\varepsilon(x_2) = 1 - \frac{\varepsilon}{2}\left(\frac{x_2^2}{h^2} - \frac{1}{3}\right) + \frac{\varepsilon^2}{24}\left(\frac{x_2^4}{h^4} + 2\frac{x_2^2}{h^2} - \frac{13}{15}\right),$$

$$w_\varepsilon(x_2) = 1 - \frac{\varepsilon}{4}\left(\frac{x_2^2}{h^2} - 2\frac{x_2}{h} - \frac{1}{3}\right) + \frac{\varepsilon^2}{96}\left(\frac{x_2^4}{h^4} - 4\frac{x_2^3}{h^3} + 14\frac{x_2^2}{h^2} - 20\frac{x_2}{h} - \frac{73}{15}\right),$$

for two- and one-sided Winkler foundation, respectively. These conditions incorporate first and second order corrections to the traditional formulation of the Saint-Venant's principle at $\varepsilon = 0$, given by (100). They demonstrate that due to the presence of the Winkler foundation a self-equilibrated loading results in a small amplitude non-decaying pattern, see examples in Sections 2 and 3, in contrast to a strip with traction free semi-infinite sides.

It is obvious that within exponentially small asymptotic error, the derived decay and boundary conditions are also valid for a finite strip of length $L \gg h$, e.g., for $L \sim h\varepsilon^{-1/2}$ in accordance with the scaling adapted in Appendix. In the latter case, these conditions can be easily implemented for the edge at $x_1 \sim L$.

It is worth noting that the developed framework is not restricted to the considered scalar problem in linear elasticity for a semi-infinite strip in contact with the simplest Winkler foundation. It may be extended to a broad range of the problems for thin elastic structures interacting with softer environment. In particular, plane and 3D problems for a layer resting on a deformable foundation can be treated in a similar manner, including a low frequency dynamic behaviour as well as heat and mass transfer through thin layers and coatings. Novel amendments of the canonical Saint-Venant's principle will likely follow from the mentioned considerations.

## CRediT authorship contribution statement

**Ludmila Prikazchikova:** Writing – original draft, Validation, Software, Investigation, Formal analysis. **Evgeniya Nolde:** Writing – review & editing, Validation, Software, Investigation, Formal analysis, Data curation. **Wiktoria Miszuris:** Writing – review & editing, Methodology, Formal analysis, Conceptualization. **Julius Kaplunov:** Writing – review & editing, Supervision, Methodology, Conceptualization.

## Declaration of competing interest

The authors declare that they have no known competing financial interests or personal relationships that could have appeared to influence the work reported in this paper.

## Data availability

No data was used for the research described in the article.

## Acknowledgements

LP, JK and WM are thankful to the H2020-MSCA-RISE project 'EffectFact' ID: 101008140 and their secondment industrial hosts (ROEZ, Slovakia and CAEmate, Italy) for the hospitality. LP was supported by the Engineering and Physical Sciences Research Council, UK [EP/Y021983/1]. WM also acknowledges partial support from the project within the Innovate Ukraine competition, funded by UK International Development and hosted by British Embassy Kyiv.

## Appendix. Asymptotic derivation of higher order equilibrium equations

Consider antiplane shear of an elastic strip of thickness $2h$, interacting with a Winkler-type foundation along both horizontal sides, see Fig. 1. In what follows, we study long-wave deformation along the $x_1$-axis in order to deduce an approximate 1D equation for the mid-strip displacement. Thus, we define here different scaling along $x_1$- and $x_2$-axes, keeping in mind that $\partial/\partial x_1 \ll \partial/\partial x_2$. More specifically, we assume that $\partial/\partial x_1 \sim \sqrt{\varepsilon}\partial/\partial x_2$, where the small parameter $\varepsilon$ is given by (13). Instead of dimensionless variables $\xi$ in (16) we use here another variable $\chi$, expressed as

$$\chi = \frac{x_1\sqrt{\varepsilon}}{h}, \tag{A.1}$$

keeping the second variable $\zeta$ the same as in the main part of the paper.

The governing Eq. (1) can now be written in term of dimensionless displacement $u^*$, see (17), as follows

$$\varepsilon\frac{\partial^2 u^*}{\partial\chi^2} + \frac{\partial^2 u^*}{\partial\zeta^2} = 0, \tag{A.2}$$

subject to boundary condition (23). We look for the asymptotic series in the form

$$u^*(\chi,\zeta) = u^{(0)}(\chi,\zeta) + \varepsilon u^{(2)}(\chi,\zeta) + \varepsilon^2 u^{(4)}(\chi,\zeta) + \cdots, \tag{A.3}$$

where

$$u^{(2n)}(\chi,\zeta) = \sum_{m=0}^{n} \zeta^{2m} u_{2m}^{(2n)}(\chi), \qquad n = 0,1,2,\dots. \tag{A.4}$$

Further detail on the adapted asymptotic technique can be found in Goldenveizer et al. (1993). By substituting (A.3) into (A.2), and combining terms with the same powers of $\varepsilon$, we get

$$\frac{\partial^2 u^{(2n)}}{\partial\chi^2} + \frac{\partial^2 u^{(2n+2)}}{\partial\zeta^2} = 0, \qquad n = 0,1,2,\dots.$$

Taking into account (A.4), the last equation reduces to

$$\sum_{m=0}^{n} \zeta^{2m}\left(\frac{d^2 u_{2m}^{(2n)}}{\partial\chi^2} + 2(m+1)(2m+1)u_{2m+2}^{(2n+2)}\right) = 0, \qquad n = 0,1,2,\dots. \tag{A.5}$$

Then, from the boundary condition (20) we have

$$\sum_{m=1}^{n} 2\, m u_{2m}^{(2n)} = -\sum_{m=0}^{n-1} u_{2m}^{(2n-2)}, \qquad n = 1,2,\dots. \tag{A.6}$$

It is now convenient to rewrite Eqs. (A.5) and (A.6) as

$$\frac{d^2 u_0^{(2n)}}{d\chi^2} + 2u_2^{(2n+2)} = 0, \qquad n = 0,1,2,\dots, \tag{A.7}$$

$$u_{2m}^{(2n)} = -\frac{1}{2m(2m-1)}\frac{d^2 u_{2m-2}^{(2n-2)}}{d\chi^2}, \qquad n = 2,3,\dots, \quad m = 2,3,\dots,n, \tag{A.8}$$

and

$$u_2^{(2)} = -\frac{1}{2}u_0^{(0)}, \quad u_2^{(2n+2)} = -\sum_{m=2}^{n+1} m u_{2m}^{(2n+2)} - \frac{1}{2}\sum_{m=0}^{n} u_{2m}^{(2n)}, \qquad n = 1,2,\dots. \tag{A.9}$$

From (A.7) at $n = 0$ and $(A.9)_1$, we arrive at a differential equation for $u_0^{(0)}$, given by

$$\frac{d^2 u_0^{(0)}}{d\chi^2} - u_0^{(0)} = 0. \tag{A.10}$$

Next, using (A.7)–(A.10), we can express $u_{2i}^{(2n)}$, $i = 1,\dots,n$, in terms of $u_0^{(2j-2)}$, $j = 2,\dots,n$, $n \geq 2$. In particular, we obtain

$$\frac{d^2 u_0^{(2)}}{d\chi^2} - u_0^{(2)} + \frac{1}{3}u_0^{(0)} = 0, \qquad \frac{d^2 u_0^{(4)}}{d\chi^2} - u_0^{(4)} + \frac{1}{3}u_0^{(2)} - \frac{4}{45}u_0^{(0)} = 0, \tag{A.11}$$

and

$$u_2^{(4)} = -\frac{1}{2}u_0^{(2)} + \frac{1}{6}u_0^{(0)}, \quad u_4^{(4)} = \frac{1}{24}u_0^{(0)}. \tag{A.12}$$

Combining (A.10)–(A.11), we have the following 1D equation for the dimensionless mid-strip displacement $U^* = u^*\big|_{\zeta=0} = u_0^{(0)} + \varepsilon u_0^{(2)} + \varepsilon^2 u_0^{(4)} + \cdots$

$$\frac{d^2 U^*}{d\chi^2} - \left(1 - \frac{1}{3}\varepsilon + \frac{4}{45}\varepsilon^2 + \cdots\right)U^* = 0. \tag{A.13}$$

In addition, from (A.9), (A.12), (A.3), (A.4), and also (2), we derive the expressions for dimensional displacement and shear stresses in terms of $U = hU^*$. Keeping $O(\varepsilon^2)$ terms we get

$$\begin{aligned} u &= \left[1 - \frac{1}{2}\varepsilon\zeta^2 + \varepsilon^2\left(\frac{1}{6}\zeta^2 + \frac{1}{24}\zeta^4\right)\right]U, \\ \sigma_{31} &= \mu\left[1 - \frac{1}{2}\varepsilon\zeta^2 + \varepsilon^2\left(\frac{1}{6}\zeta^2 + \frac{1}{24}\zeta^4\right)\right]\frac{dU}{dx_1}, \\ \sigma_{32} &= \frac{\mu}{h}\left[-\varepsilon\zeta + \varepsilon^2\left(\frac{1}{3}\zeta + \frac{1}{6}\zeta^3\right)\right]U. \end{aligned} \tag{A.14}$$

Suppose now that a strip is supported by a Winkler foundation along the side $x_2 = -h$ only, see Fig. 2. In this case, instead of boundary conditions (3) we use (63). We look for solution of (A.2), (65) in the form (A.3), where

$$u^{(2n)}(\chi,\zeta) = \sum_{k=0}^{n}\zeta^k u_k^{(2n)}(\chi), \qquad n = 0,1,2,\dots. \tag{A.15}$$

By substituting (A.3) into (A.2) and taking into account (A.15), we obtain

$$\sum_{k=0}^{2n}\zeta^k\left(\frac{d^2u_k^{(2n)}}{\partial\chi^2} + (k+1)(k+2)u_{k+2}^{(2n+2)}\right) = 0, \qquad n = 0,1,2,\dots. \tag{A.16}$$

From boundary conditions (65) we have

$$\sum_{k=1}^{2n} k u_k^{(2n)} = 0, \qquad \sum_{k=1}^{2n}(-1)^{k+1}k u_k^{(2n)} = \sum_{k=0}^{2n-2}(-1)^k u_k^{(2n-2)}, \qquad n = 1,2,\dots. \tag{A.17}$$

We can rewrite (A.16) and (A.17) as

$$\frac{d^2u_0^{(2n)}}{d\chi^2} + 2u_2^{(2n+2)} = 0, \qquad n = 0,1,2,\dots, \tag{A.18}$$

$$u_k^{(2n)} = -\frac{1}{k(k-1)}\frac{d^2u_{k-2}^{(2n-2)}}{d\chi^2}, \qquad n = 2,3,\dots,\quad k = 2,3,\dots,n, \tag{A.19}$$

and

$$\begin{aligned} u_1^{(2)} &= \frac{1}{2}u_0^{(0)}, \quad u_1^{(2n)} = -\sum_{k=2}^{n}(2k-1)u_{2k-1}^{(2n)} + \frac{1}{2}\sum_{k=0}^{2n-2}(-1)^k u_k^{(2n-2)}, \\ u_2^{(2)} &= -\frac{1}{4}u_0^{(0)}, \quad u_2^{(2n)} = -\sum_{k=2}^{n}k u_{2k}^{(2n)} - \frac{1}{4}\sum_{k=0}^{2n-2}(-1)^k u_k^{(2n-2)}. \end{aligned} \tag{A.20}$$

where $n = 2,3,\dots$. By using the equations above, we can express $u_k^{(2n)}$, $n = 1,2,\dots$, $k = 1,\dots,2n$, in terms of $u_0^{(2j-2)}$, $j = 2,\dots,n$. In particular, we have

$$\begin{aligned} &\frac{d^2u_0^{(0)}}{d\chi^2} - \frac{1}{2}u_0^{(0)} = 0, \quad \frac{d^2u_0^{(2)}}{d\chi^2} - \frac{1}{2}u_0^{(2)} + \frac{1}{3}u_0^{(0)} = 0, \\ &\frac{d^2u_0^{(4)}}{d\chi^2} - \frac{1}{2}u_0^{(4)} + \frac{1}{3}u_0^{(2)} - \frac{8}{45}u_0^{(0)} = 0, \end{aligned} \tag{A.21}$$

and

$$u_1^{(4)} = \frac{1}{2}u_0^{(2)} - \frac{1}{4}u_0^{(0)}, \quad u_2^{(4)} = -\frac{1}{4}u_0^{(2)} + \frac{1}{6}u_0^{(0)}, \quad u_3^{(4)} = -\frac{1}{24}u_0^{(0)}, \quad u_4^{(4)} = \frac{1}{96}u_0^{(0)}.$$

Keeping $O(\varepsilon^2)$ terms, we arrive at

$$\frac{d^2U^*}{d\chi^2} - \left(\frac{1}{2} - \frac{1}{3}\varepsilon + \frac{8}{45}\varepsilon^2\right)U^* = 0. \tag{A.22}$$

Then, the dimensional displacement and shear stresses are given by

$$\begin{aligned} u &= \left[1 + \varepsilon\left(\frac{1}{2}\zeta - \frac{1}{4}\zeta^2\right) + \varepsilon^2\left(-\frac{1}{4}\zeta + \frac{1}{6}\zeta^2 - \frac{1}{24}\zeta^3 + \frac{1}{96}\zeta^4\right)\right]U, \\ \sigma_{31} &= \mu\left[1 + \varepsilon\left(\frac{1}{2}\zeta - \frac{1}{4}\zeta^2\right) + \varepsilon^2\left(-\frac{1}{4}\zeta + \frac{1}{6}\zeta^2 - \frac{1}{24}\zeta^3 + \frac{1}{96}\zeta^4\right)\right]\frac{dU}{dx_1}, \\ \sigma_{32} &= \frac{\mu}{h}\left[\varepsilon\frac{1}{2}(1-\zeta) + \varepsilon^2\left(-\frac{1}{4} + \frac{1}{3}\zeta - \frac{1}{8}\zeta^2 + \frac{1}{24}\zeta^3\right)\right]U. \end{aligned} \tag{A.23}$$

## References

Aghalovyan, L. A. (2015). *Asymptotic theory of anisotropic plates and shells*. World Scientific.
Argatov, I., & Mishuris, G. (2015). *Contact mechanics of articular cartilage layers. Asymptotic models*. Springer.

Atkinson, K. (1991). *An introduction to numerical analysis*. John Wiley & Sons.

Babenkova, E., & Kaplunov, J. (2004). Low–frequency decay conditions for a semi–infinite elastic strip. *Proceedings of the Royal Society of London. Series A. Mathematical, Physical and Engineering Sciences*, *460*(2048), 2153–2169.

Barber, J. R. (2018). *Contact mechanics*. Springer.

Erbaş, B., Kaplunov, J., & Elishakoff, I. (2022). Asymptotic derivation of a refined equation for an elastic beam resting on a Winkler foundation. *Mathematics and Mechanics of Solids*, *27*(9), 1638–1648.

Erbaş, B., Kaplunov, J., & Kiliç, G. (2022a). Asymptotic analysis of 3D dynamic equations in linear elasticity for a thin layer resting on a Winkler foundation. *IMA Journal of Applied Mathematics*, *87*(5), 707–721.

Erbaş, B., Kaplunov, J., Nobili, A., & Kılıç, G. (2018). Dispersion of elastic waves in a layer interacting with a Winkler foundation. *Journal of the Acoustical Society of America*, *144*(5), 2918–2925.

Falope, F. O., Lanzoni, L., & Radi, E. (2022). 2D Green's functions for an elastic layer on a rigid support loaded by an internal point force. *International Journal of Engineering Science*, *173*, Article 103652.

Frỳba, L. (2013). *vol. 1*, *Vibration of solids and structures under moving loads*. Springer Science & Business Media.

Fuss, N. (1793). *Versuch einer Theorie des Widerstandes zwey- und vierrädriger Fuhrwerke auf Fahrwegen jeder Art; mit Bestimmung der Umstände, unter welchen die einen vor den andern den Vorzug verdienen*. Friedrich Brummer.

Gholami, R., & Ansari, R. (2017). A unified nonlocal nonlinear higher-order shear deformable plate model for postbuckling analysis of piezoelectric-piezomagnetic rectangular nanoplates with various edge supports. *Composite Structures*, *166*, 202–218.

Goldenveizer, A. (1976). *Theory of Thin Elastic Shells*. Izdatel'stvo Nauka: (In Russian).

Goldenveizer, A. (1994). Algorithms of the asymptotic construction of linear two-dimensional thin shell theory and the St Venant principle. *Journal of Applied Mathematics and Mechanics*, *58*(6), 1039–1050.

Goldenveizer, A. (1998). The boundary conditions in the two-dimensional theory of shells. The mathematical aspect of the problem. *Journal of Applied Mathematics and Mechanics*, *62*(4), 617–629.

Goldenveizer, A. L. (2014). *vol. 2*, *Theory of elastic thin shells: solid and structural mechanics*. Elsevier.

Goldenveizer, A., Kaplunov, J., & Nolde, E. (1993). On Timoshenko-Reissner type theories of plates and shells. *International Journal of Solids and Structures*, *30*(5), 675–694.

Gregory, R. D., & Wan, F. Y. (1984). Decaying states of plane strain in a semi-infinite strip and boundary conditions for plate theory. *Journal of Elasticity*, *14*(1), 27–64.

Gregory, R., & Wan, F. (1985). On plate theories and Saint-Venant's principle. *International Journal of Solids and Structures*, *21*(10), 1005–1024.

Gusein-Zade, M. (1965). On necessary and sufficient conditions for the existence of decaying solutions of the plane problem of the theory of elasticity for a semistrip. *Journal of Applied Mathematics and Mechanics*, *29*(4), 892–901.

Kaplunov, J., Erbaş, B., & Ege, N. (2022). Asymptotic derivation of 2D dynamic equations of motion for transversely inhomogeneous elastic plates. *International Journal of Engineering Science*, *178*, Article 103723.

Kaplunov, J. D., Kossovich, L. Y., & Nolde, E. (1998). *Dynamics of thin walled elastic bodies*. Academic Press.

Kaplunov, J., Prikazchikov, D. A., Rogerson, G. A., & Lashab, M. I. (2014). The edge wave on an elastically supported Kirchhoff plate. *Journal of the Acoustical Society of America*, *136*(4), 1487–1490.

Kaplunov, J., Prikazchikov, D., & Sultanova, L. (2018). Justification and refinement of Winkler–Fuss hypothesis. *Zeitschrift für angewandte Mathematik und Physik*, *69*, 1–15.

Kaplunov, J., Prikazchikova, L., & Alkinidri, M. (2021). Antiplane shear of an asymmetric sandwich plate. *Continuum Mechanics and Thermodynamics*, *33*, 1247–1262.

Krasnitckii, S., Smirnov, A., & Gutkin, M. Y. (2023). Misfit stress and energy in composite nanowire with polygonal core. *International Journal of Engineering Science*, *193*, Article 103959.

Li, P., Li, W., Tan, Y., Fan, H., & Wang, Q. (2024). A phase field fracture model for ultra-thin micro-/nano-films with surface effects. *International Journal of Engineering Science*, *195*, Article 104004.

Lou, M., Wang, H., Chen, X., & Zhai, Y. (2011). Structure–soil–structure interaction: Literature review. *Soil Dynamics and Earthquake Engineering*, *31*(12), 1724–1731.

Love, A. E. H. (2013). *A treatise on the mathematical theory of elasticity*. Cambridge University Press.

Malikan, M. (2024). On mechanics of piezocomposite shell structures. *International Journal of Engineering Science*, *198*, Article 104056.

Marušić-Paloka, E., & Pažanin, I. (2022). The effective boundary condition on a porous wall. *International Journal of Engineering Science*, *173*, Article 103638.

Mathúna, D. Ó. (1989). Plate theory and the edge effects. *Mechanics, Boundary Layers and Function Spaces*, 73–140.

Matysiak, S., & Pauk, V. (2003). Edge crack in an elastic layer resting on Winkler foundation. *Engineering Fracture Mechanics*, *70*(17), 2353–2361.

Mishuris, G., Miszuris, W., & Öchsner, A. (2007a). Evaluation of transmission conditions for a thin heat-resistant inhomogeneous interphase in dissimilar material. In *Materials science forum*: *vol. 553*, (pp. 87–92). Trans Tech Publ.

Mishuris, G., Miszuris, W., & Öchsner, A. (2007b). Finite element verification of transmission conditions for 2D heat conduction problems. In *Materials science forum*: *vol. 553*, (pp. 93–99). Trans Tech Publ.

Mishuris, G., & Öchsner, A. (2005). Edge effects connected with thin interphases in composite materials. *Composite Structures*, *68*(4), 409–417.

Mishuris, G., Ochsner, A., Kuhn, G., La Rocca, A., Power, H., La Rocca, V., et al. (2005). FEM-analysis of nonclassical transmission conditions between elastic structures part 1: soft imperfect interface. *CMC-TECH SCIENCE PRESS-*, *2*(4), 227.

Miszuris, W., & Öchsner, A. (2013). Universal transmission conditions for thin reactive heat-conducting interphases. *Continuum Mechanics and Thermodynamics*, *25*, 1–21.

Prikazchikova, L. (2022). Decay conditions for antiplane shear of a high-contrast multi-layered semi-infinite elastic strip. *Symmetry*, *14*(8), 1697.

Shugailo, T., Nobili, A., & Mishuris, G. (2023). A mechanical model for thin sheet straight cutting in the presence of an elastic support. *International Journal of Engineering Science*, *193*, Article 103964.

Sonato, M., Piccolroaz, A., Miszuris, W., & Mishuris, G. (2015). General transmission conditions for thin elasto-plastic pressure-dependent interphase between dissimilar materials. *International Journal of Solids and Structures*, *64*, 9–21.

Stempin, P., Pawlak, T. P., & Sumelka, W. (2023). Formulation of non-local space-fractional plate model and validation for composite micro-plates. *International Journal of Engineering Science*, *192*, Article 103932.

Wan, F. Y. (2000). Outer solution for elastic torsion by the method of boundary layer residual states. *Zeitschrift für angewandte Mathematik und Physik ZAMP*, *51*, 509–529.

Wilde, M. V., Surova, M. Y., & Sergeeva, N. V. (2022). Asymptotically correct boundary conditions for the higher-order theory of plate bending. *Mathematics and Mechanics of Solids*, *27*(9), 1813–1854.

Winkler, E. (1867). *Die Lehre von der Elastizität und Festigkeit*. Dominicus, Prag.

Zimmermann, H. (1888). Calculation of the upper surface construction of railway tracks. Berlin, Ernst and Korn Verlag.